JGP Journal of General Physiology

ARTICLE

The versatile regulation of K_{2P} channels by polyanionic lipids of the phosphoinositide and fatty acid metabolism

Elena B. Riel[1*], Björn C. Jürs[1,2*], Sönke Cordeiro[1], Marianne Musinszki[1], Marcus Schewe[1a], and Thomas Baukrowitz[1b]

Work over the past three decades has greatly advanced our understanding of the regulation of K_{ir} K^+ channels by polyanionic lipids of the phosphoinositide (e.g., PIP_2) and fatty acid metabolism (e.g., oleoyl-CoA). However, comparatively little is known regarding the regulation of the K_{2P} channel family by phosphoinositides and by long-chain fatty acid–CoA esters, such as oleoyl-CoA. We screened 12 mammalian K_{2P} channels and report effects of polyanionic lipids on all tested channels. We observed activation of members of the TREK, TALK, and THIK subfamilies, with the strongest activation by PIP_2 for TRAAK and the strongest activation by oleoyl-CoA for TALK-2. By contrast, we observed inhibition for members of the TASK and TRESK subfamilies. Our results reveal that TASK-2 channels have both activatory and inhibitory PIP_2 sites with different affinities. Finally, we provided evidence that PIP_2 inhibition of TASK-1 and TASK-3 channels is mediated by closure of the recently identified lower X-gate as critical mutations within the gate (i.e., L244A, R245A) prevent PIP_2-induced inhibition. Our findings establish that K^+ channels of the K_{2P} family are highly sensitive to polyanionic lipids, extending our knowledge of the mechanisms of lipid regulation and implicating the metabolism of these lipids as possible effector pathways to regulate K_{2P} channel activity.

Introduction

Members of the large family of two-pore domain potassium (K_{2P}) channels are critically involved in many cellular functions ranging from renal ion homeostasis, cell development, hormone secretion, and immune functions as well as cardiac and neuronal excitability (Enyedi and Czirják, 2010). Accordingly, dysregulation of K_{2P} channels is seen in many disease states, such as cardiac disorders (i.e., atrial fibrillation, ventricular tachycardia; Liang et al., 2014; Decher et al., 2017b), hyperaldosteronism (Davies et al., 2008; Bandulik et al., 2015), and pulmonary arterial hypertension (Olschewski et al., 2006; Ma et al., 2013; Antigny et al., 2016), as well as in pain perception disorders, such as migraine and depression (Alloui et al., 2006; Heurteaux et al., 2006; Lafrenière et al., 2010; Andres-Enguix et al., 2012; Royal et al., 2019). Initially thought to mediate passive background conductance in excitable cells, increasing evidence shows that K_{2P} channels are highly regulated by sensing a broad range of diverse physiological stimuli and endogenous ligands. However, not all K_{2P} channels respond to the same set of stimuli; rather, their sensitivity profile corresponds to their affiliation with one of the known six subfamilies (TREK, TASK, TALK, THIK, TWIK, and TRESK). Members of the TREK subfamily (TREK-1, TREK-2, and TRAAK) display the most diverse (and, e.g., regarding TREK-1, the best investigated) regulation, with relevant stimuli including temperature (Maingret et al., 2000a), mechanical force (Maingret et al., 1999; Chemin et al., 2005), membrane voltage (Maingret et al., 2002; Schewe et al., 2016), extracellular/intracellular pH (Maingret et al., 1999; Honoré et al., 2002), partner proteins (Plant et al., 2005; Sandoz et al., 2006), and various lipids (Maingret et al, 2000b; Chemin et al, 2005, 2007). Members of the TALK subfamily (TASK-2, TALK-1, and TALK-2) are activated by high extracellular pH (Morton et al., 2003; Duprat et al., 2005; Niemeyer et al., 2010). TASK-1, TASK-3, and TASK-5 make up the TASK subfamily, and members are inhibited by extracellular acidification (Rajan et al., 2000; Bayliss et al., 2001; Morton et al., 2003) but also respond to membrane lipids such as diacylglycerol (DAG; Wilke et al., 2014). Members of the TWIK subfamily (TWIK-1, TWIK-2, and TWIK-3) are rather stimuli insensitive, but their cellular activity is controlled by regulated protein trafficking (Feliciangeli et al., 2007;

[1]Institute of Physiology, Kiel University, Kiel, Germany; [2]Medical School Hamburg, University of Applied Sciences and Medical University, Hamburg, Germany.

*E.B. Riel and B.C. Jürs contributed equally to this paper; Correspondence to Marcus Schewe: m.schewe@physiologie.uni-kiel.de; Thomas Baukrowitz: t.baukrowitz@physiologie.uni-kiel.de.

Feliciangeli et al., 2010) as well as possibly SUMOylation (Rajan et al., 2005; Plant et al., 2010) and unique features of the selectivity filter (SF) gate (Nematian-Ardestani et al., 2020). The TRESK subfamily has just one member (i.e., TRESK) and is regulated in particular by changes in intracellular Ca^{2+} levels mediated by the calmodulin-dependent phosphatase calcineurin (Czirják et al., 2004). For the THIK subfamily (THIK-1 and THIK-2), no physiological gating stimulus has been reported so far.

Work of the last three decades revealed that many ion channels are regulated by phosphoinositides and in particular by the most abundant phosphoinositide, phosphoinositol-4,5-bisphosphate ($PI(4,5)P_2$; PIP_2). PIP_2-sensitive channels include all members of the inward-rectifying potassium (K_{ir}) channels (Suh and Hille, 2005; Logothetis et al., 2007; Suh and Hille, 2008) but also members of the voltage-gated potassium (K_v) channels (Oliver et al., 2004; Rodriguez et al., 2010; Kruse et al., 2012; Zaydman and Cui, 2014; Taylor and Sanders, 2017), transient receptor potential (TRP) cation channels (Qin, 2007; Suh and Hille, 2008), Ca^{2+}-activated BK-type channels (Vaithianathan et al., 2008), hyperpolarization-activated and cyclic nucleotide–gated channels (Pian et al., 2006; Zolles et al., 2006; Ying et al., 2011), and a number of ion transporters (i.e., NCX, NCE, PMCA; Hilgemann et al., 2001; Gamper and Shapiro, 2007). Many physiologically important processes, such as insulin secretion in pancreatic β-cells (Rorsman and Ashcroft, 2018) or mechanical transduction and adaptation in hair cells (Hirono et al., 2004; Effertz et al., 2017), involve the regulation of ion channels by phosphoinositides. The mechanisms of regulation in some of these channels have been resolved to the atomic level (Hansen et al., 2011; Niu et al., 2020; Sun and MacKinnon, 2020).

The first report on the regulation of a K_{2P} channel by phosphoinositides dates to 2005 and still represents an important reference on this topic (Chemin et al., 2005). Chemin and colleagues reported the strong activation of TREK-1 channels by several phospholipids, including phosphatidylethanolamine, phosphatidylinositol, phosphatidylserine, phosphatidic acid (PA), and PIP_2 (with PA being the most potent lipid), and identified a cluster of basic residues in the proximal C-terminus directly extending from TM4 as a potential PIP_2 binding region (Chemin et al., 2005). Accordingly, it was proposed that negatively charged lipids (e.g., PIP_2) electrostatically interact with these clustered basic residues and thereby cause channel activation (Chemin et al., 2005). Later the same authors reported that PIP_2 application can also produce TREK-1 inhibition (Chemin et al, 2007). More recently, an additional potential PIP_2 interaction region in the more distal C-terminus of TREK-1 channels has been suggested (Soussia et al., 2018). The direct binding of anionic lipids such as PA, phosphatidylglycerol (PG), and PIP_2 to purified TREK-1 channels was demonstrated via a fluorescence binding assay (Cabanos et al., 2017) and to purified TRAAK channels by means of mass spectrometry (Schrecke et al., 2021). Furthermore, TREK-1 was shown to bind phospholipase D2 (PLD2) via its C-terminus and the local production of PA by PLD2 to produce channel activation. Interestingly, Cabanos and colleagues reported that PIP_2 can displace PA and PG in TREK-1 to produce channel inhibition as measured in a liposome K^+ flux assay (Cabanos et al., 2017).

Aside from the TREK subfamily, the effects of PIP_2 have also been studied in TASK-1, TASK-2, TASK-3, and TRESK channels. Initially, the inhibition of TASK-1 and TASK-3 by phospholipase C (PLC) activation was thought to result from PIP_2 breakdown (Lopes et al., 2005), as PIP_2 appeared to cause activation; however, later it became clear that DAG (released by PLC) likely inhibits TASK-1 and TASK-3 channels directly (Wilke et al., 2014). In TASK-2 channels and human (but not rodent) TRESK channels, application of PIP_2 to excised patches has been reported to cause activation (Lopes et al., 2005; Niemeyer et al., 2017; Giblin et al., 2019).

Another class of polyanionic lipids known to regulate ion channels are long-chain fatty acid coenzyme A (LC-CoA) esters. These obligate metabolites of cellular fatty acids affect many K_{ir} channels, producing activation in K_{ATP} ($K_{ir}6.2$/SUR) channels (Bränström et al., 1998; Schulze et al., 2003) but inhibition in most other K_{ir} channels (Rapedius et al., 2005; Shumilina et al., 2006; Tucker and Baukrowitz, 2008; Cheng et al., 2011). Aside from the K_{ir} channel family, little is known about the effects of LC-CoA on other ion channels. However, TRPV1 channels have been reported to be activated by LC-CoA (Yu et al., 2014). In both, K_{ir} channels and TRPV1, LC-CoA appears to interact with the same sites that also bind PIP_2, likely via the negative phosphate groups present in both types of lipids (Schulze et al., 2003; Yu et al., 2014).

Aside from the aforementioned exception of TREK/TRAAK, TASK-1/-2/-3, and TRESK channels, effects of phosphoinositides on other members of the K_{2P} channel family have not been investigated yet, and K_{2P} channel regulation by LC-CoA is so far unexplored. Therefore, we systematically studied the effect of PIP_2 and LC-CoA on K_{2P} channels by testing all functionally expressing channels (12 out of 15) under identical conditions and quantified their respective sensitivities. We uncovered that all K_{2P} channel members strongly respond to at least one of the two polyanionic lipid species and that the six K_{2P} channel subfamilies can be classified as either polyanionic lipid-activated or lipid-inhibited subfamilies. Furthermore, we investigated the physicochemical prerequisites for lipid activation in TALK-2 channels and the structural regulation mechanism of lipid regulation in the TASK subfamily. We finally discuss the potential physiological relevance of our findings that, however, warrant further investigation in more native preparations.

Materials and methods

Molecular biology and oocyte expression

For this study, we used the coding sequences of hTWIK-1 (GenBank accession no. NM_002245.3), hTREK-1 (NM_172042.2), rTREK-1 (NM_172041.2), hTREK-2 (NM_138318.2), hTRAAK (AF_247042.1), hTALK-1 (NM_032115.4), hTALK-2 (EU978944.1), hTASK-2 (NM_003740.3), hTASK-1 (NM_002246.2), hTASK-3 (XM_011517102.1), hTHIK-1 (NM_022054), hTHIK-2 (NM_022055.1), and hTRESK (NM_181840.1). To increase surface expression and macroscopic currents, measurements of TWIK-1 and THIK-2 channels were performed using channels with

mutated retention motifs and a known activating mutation hTHIK-2, respectively (TWIK-1 I293A/I294A [TWIK-1*] and THIK-2 R11A/R12A/R14A/R15A/R16A/A155P [THIK-2*]). All mutant channels were obtained by site-directed mutagenesis with custom oligonucleotides. All constructs were subcloned into the pFAW dual-purpose vector suitable for in vitro transcription/oocyte expression and transfection of cultured cells and verified by sequencing. cRNA was synthetized using AmpliCap-Max T7 or SP6 High Yield Message Maker Kits (CELLSCRIPT) and stored at −20°C (for frequent use) and −80°C (for long-term storage). *Xenopus laevis* oocytes were surgically removed from adult female frogs and treated with type II collagenase before manual defolliculation. Oocytes were injected with ∼50 nl of channel-specific cRNA (0.5–1 µg µl^{-1}) and incubated at 17°C for 1–14 d before experimental use.

Cell culture

HEK293 cells were cultured in DMEM, supplemented with 10% FCS and 10 U ml^{-1} penicillin and 10 mg ml^{-1} streptomycin in a 5% CO_2 atmosphere at 37°C. The cells were transiently transfected with Lipofectamine 2000 (Invitrogen) in 24-well plates. For electrophysiological recordings, the transfected cells were trypsinized at least 4 h before electrophysiological measurements and seeded onto sterile 10-mm coverslips in 35-mm culture dishes in antibiotic-free DMEM.

Electrophysiology

Currents were recorded from inside-out membrane patches excised from cRNA-injected *Xenopus* oocytes or from transiently transfected HEK293 cells at room temperature (21–23°C). For oocyte measurements, pipettes were made from thick-walled borosilicate glass capillaries and had resistances of 0.3–0.8 MΩ. Pipettes were filled with a standard pipette solution (in mM): 120 KCl, 10 HEPES, and 3.6 $CaCl_2$, pH 7.4, adjusted with KOH/HCl. Currents were recorded using an EPC9 or EPC10 amplifier (HEKA Elektronik), sampled at 10 kHz, and filtered with 3 kHz (−3 dB). The recording program was PATCHMASTER (HEKA Elektronik; version v2×73.5). The used pulse protocols were either ramps ranging from −80 to +40 or +80 mV with a duration of 1 s and intervals of 4 or 9 s, or measurements were performed using a continuous pulse at +40 mV. Solutions were applied to the cytoplasmic side of excised membrane patches via a gravity flow multibarrel application system. Standard intracellular (bath) solutions were composed of (in mM): 120 KCl, 10 HEPES, 2 EGTA, and 1 pyrophosphate; pH was adjusted to pH 7.4 with KOH/HCl. 5 mg ml^{-1} BSA was added to obtain washout solution. Where indicated in experimental results, 120 mM KCl was replaced by 120 mM RbCl.

HEK293 cell measurements were performed in the whole-cell configuration of the patch-clamp technique using an EPC10 amplifier (HEKA Elektronik) and PATCHMASTER software (HEKA Elektronik; version v2×73.5) with a sampling rate and filter as above. The cells were stimulated by a ramp protocol from −100 to +60 mV with 1-s duration and a 5-s interpulse duration. Pipette resistances ranged from 1 to 3 MΩ, and pipettes were filled with intracellular solution (in mM): 140 KCl, 2 $MgCl_2$, 1 $CaCl_2$, 2.5 EGTA, and 10 HEPES, pH 7.3, adjusted with KOH/HCl. The bath contained (in mM): 135 NaCl, 5 KCl, 2 $MgCl_2$, 2 $CaCl_2$, 10 glucose, and 10 HEPES, pH 7.3, adjusted with NaOH/HCl. All modifying reagents were added directly to the bath to obtain the particular end concentrations. Lipids and other substances were stored as stock solutions (1–100 mM) at −20°C and diluted in the bath solution to the final concentration before measurements.

Chemicals, drugs, and lipids

LC-CoA (14:0, 16:0, 18:0, 18:1, 18:2, 18:3, 22:0) were purchased from Avanti Polar Lipids (Alabaster), and stock solutions were prepared in DMSO (1–5 mM). The PLC activator m-3m3FBS, tetrapentylammonium chloride, and L-α-PI(4,5)P_2 ammonium salt (brain PI(4,5)P_2, PIP_2) were purchased from Sigma-Aldrich/Merck, and stock solutions were prepared in DMSO (1–100 mM).

Animals (*Xenopus*)

The performed investigation conforms to the Guide for the Care and Use of Laboratory Animals (National Institutes of Health Publication No. 85-23). For this study, we used female *Xenopus* animals (n = 25) that were accommodated at the animal breeding facility of the Christian Albrecht University of Kiel to isolate oocytes. Experiments using *Xenopus* toads were approved by the local ethics commission.

Data analysis

Data analysis was performed using FITMASTER (HEKA Elektronik; version v2×73.5), Microsoft Excel, and Igor Pro (version 6.3.7.2; Wavemetrics Inc.).

Recorded currents were analyzed from stable membrane patches at a voltage of +40 mV unless stated otherwise.

The fold activation of a ligand (drug or bioactive lipid) was calculated from the following equation:

$$\text{Fold activation (FA)} = \frac{I_{Activated}}{I_{basal}},$$

with $I_{Activated}$ representing the stable current level in the presence of a given concentration of a respective ligand and I_{basal} the measured current before ligand application.

Percentage inhibition of a ligand (drug or bioactive lipid) was calculated from stable currents of excised membrane patches using the following equation:

$$\%\ \text{Inhibition} = \left[1 - \left(\frac{I_{Inhibited}}{I_{basal}}\right)\right] \times 100,$$

where $I_{Inhibited}$ refers to the stable current level recorded in the presence of a given concentration of a drug or bioactive lipid and I_{basal} to the measured current before ligand application.

The macroscopic half-maximal concentration–inhibition relationship of a ligand was obtained using a modified Hill equation, depicted below:

$$\frac{I}{I_{basal}} = a + \frac{(1-a)\left(\frac{[x]}{IC_{50}}\right)^h}{1 + \frac{[x]^h}{IC_{50}}},$$

with I and I_{basal} are the currents in the absence and presence of a respective ligand, x is the concentration of the ligand,

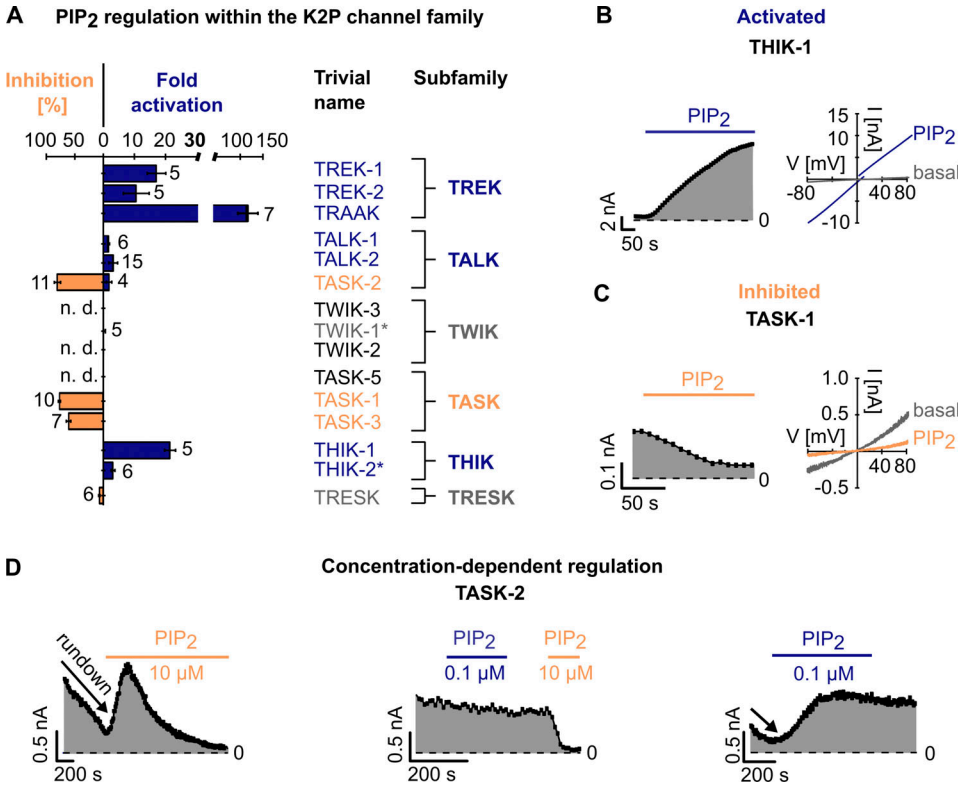

Figure 1. **PIP_2 regulation of K_{2P} channels. (A)** Fold activation (blue) and inhibition (percent; orange) of K_{2P} channel currents by 10 µM PIP_2 at +40 mV, measured in ramp protocols as shown in B and C. Insensitive channels are highlighted in gray. Number of independent experiments is indicated next to the bars. Data are summarized in Table S1. **(B and C)** Representative current traces (right) and analyzed currents at +40 mV plotted over time (left) of THIK-1 (B) and TASK-1 (C) channels measured in voltage ramps between −80 and +80 mV in excised inside-out patches of *Xenopus* oocytes using control bath solution and in the presence of 10 µM PIP_2. **(D)** Analyzed TASK-2 currents at +40 mV plotted over time, measured as in B and C, using control bath solution and in the presence of 0.1 µM or 10 µM PIP_2. Current rundown is indicated with an arrow. Low PIP_2 concentration (0.1 µM) rescues current rundown (right) but produces no inhibition (middle); 10 µM PIP_2 also rescues rundown if present (left) but leads to a subsequent inhibition of the channel. If no rundown is present, 10 µM PIP_2 only leads to inhibition (middle). All data are presented as mean ± SEM. n. d., not determined.

half-maximal inhibitory concentration is the ligand concentration at which the inhibitory effect is half maximal, h is the Hill coefficient, and a is the fraction of unblockable current (a = 0 unless stated otherwise).

Data are represented throughout the article as mean ± SEM. Significance of a respective dataset was probed with an unpaired Student's *t* test. P values are provided in the respective figures.

Image processing and figure design were performed using the open source vector graphic program Inkscape (GNU General Public License; Free Software Foundation, version 1.0.1; 3bc2e813f5, 2020-09-07; https://inkscape.org).

Online supplemental material

Fig. S1 shows the effect (activation/inhibition) of PIP_2 applied to the intracellular side of excised patches of *Xenopus* oocytes expressing K_{2P} WT and mutant channels as well as the effect of PLC-mediated PIP_2 depletion on TREK-1 channels expressed in HEK293 cells. Fig. S2 shows the effect (activation/inhibition) of oleoyl-CoA applied to inside-out patches of *Xenopus* oocytes expressing K_{2P} WT and mutant channels. Fig. S3 shows the concentration-dependent activation of TALK-2 K_{2P} channels by oleoyl-CoA in inside-out patches. Table S1, Table S2, Table S3, and Table S4 contain the numerical data points depicted graphically in Fig. 1 A, Fig. 2 A, Fig. 3 D, and Fig. 4 C, respectively.

Results

PIP_2 causes subtype-dependent responses (activation/inhibition) in most K_{2P} channels

We studied the direct effect of the most abundant phosphoinositide, $PI(4,5)P_2$ (PIP_2), on all known functionally expressing K_{2P} channels (12 in total) by applying 10 µM PIP_2 to the cytoplasmatic site of the respective channels in inside-out patches excised from *Xenopus* oocytes. The type of response (activation or inhibition) varied depending on the K_{2P} channel subfamily, and the efficacy of activation or inhibition depended on the particular subfamily member (Fig. 1 A and Table S1).

Robust PIP_2 activation was observed within the TREK subfamily with 17 ± 3-fold, 11 ± 4-fold, and 114 ± 24-fold activation for TREK-1, TREK-2, and TRAAK, respectively (Fig. 1 A). The PIP_2-activated currents displayed mildly outward-rectifying I-V relationships between −80 mV and +40 mV (Fig. S1, A–C).

Members of the THIK subfamily were also activated by PIP_2 with strong activation (19 ± twofold) for THIK-1 and weaker activation (4 ± onefold) for THIK-2*, and the activated currents

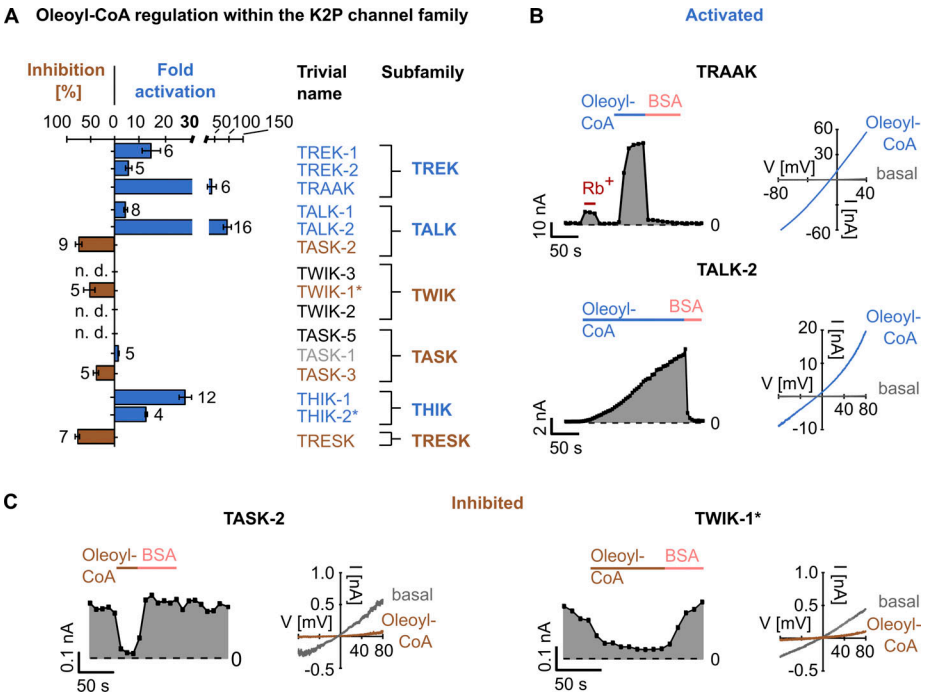

Figure 2. **Oleoyl-CoA regulation of K_{2P} channels. (A)** Fold activation (blue) and inhibition (percent; brown) of K_{2P} channels at +40 mV by 10 µM oleoyl-CoA measured as in B and C. Insensitive channels are highlighted in gray. Number of independent experiments is indicated next to the bars. Data are summarized in Table S2. **(B)** Representative current traces (right) and analyzed currents at +40 mV plotted over time (left) of TRAAK and TALK-2 channels measured in voltage ramps between −80 and +80 mV in excised inside-out patches of *Xenopus* oocytes using control bath solution and in the presence of 10 µM oleoyl-CoA or 5 mg ml^{-1} BSA. **(C)** Representative current traces of TASK-2 and TWIK-1* channels measured and analyzed as in B. All data are presented as mean ± SEM. n. d., not determined.

showed approximately linear I-V relationships (Fig. 1, A and B; Fig. S1 H). To increase surface expression, measurements of THIK-2 channels were performed using mutated channels with a removed retention motif and a point mutation in TM2 (R11A/R12A/R14A/R15A/R16A/A155P; THIK-2*; Bichet et al., 2015).

In the TALK subfamily PIP_2 caused a 4 ± 1-fold activation of TALK-2 and a weaker activation (1.7 ± 0.2-fold) of TALK-1 currents (Fig. 1 A; Fig. S1, D and E). The effect on TASK-2 was more complex and depended on the experimental history. In many excised patches, TASK-2 currents showed strong current rundown, and the application of 10 µM PIP_2 produced initially a 2.4 ± 0.3-fold activation. However, this activation ceased with time, and channel activity finally dropped below the starting level, resulting in an effective PIP_2 inhibition of 83 ± 3% (Fig. 1, A and D, left panel). In membrane patches lacking current rundown, PIP_2 application (10 µM) caused inhibition without the initial activation (Fig. 1 D, middle panel). Furthermore, lower PIP_2 concentrations (e.g., 0.1 µM) prevented current rundown (Fig. 1 D, middle panel) and activated rundown currents without producing subsequent inhibition (Fig. 1 D, right panel). These findings might indicate two distinct regulatory sites in TASK-2, with lower PIP_2 levels supporting basal channel activity via an activatory site and higher PIP_2 levels causing inhibition, possibly via a distinct inhibitory site.

In the TWIK subfamily, only TWIK-1* was expressed functionally but lacked a PIP_2 response (Fig. 1 A and Fig. S1 F). To increase surface expression, measurements of TWIK-1 were performed using channels with a mutated retention motif (TWIK-1 I293A/I294A; TWIK-1*; Bichet et al., 2015).

Likewise, no significant PIP_2 response was observed in TRESK channels (the only member of this K_{2P} channel subfamily; Fig. 1 A and Fig. S1 I), in contrast to a previous report (Giblin et al., 2019).

Finally, in the TASK subfamily, only TASK-1 and TASK-3 were expressed functionally (TASK-5 is nonfunctional; Ashmole et al., 2001), and both channels showed marked inhibition (82 ± 2% and 61 ± 4%) upon PIP_2 application (Fig. 1, A and C; Fig. S1 G).

In summary, the application of PIP_2 had effects on 10 of the 12 K_{2P} channels investigated, with only TWIK-1* and TRESK lacking any observable effect upon the addition of PIP_2. Members of the TREK, THIK, and TALK subfamilies were activated by PIP_2 (TASK-2 only initially), whereas members of the TASK subfamily were inhibited.

Most K_{2P} channels are highly sensitive to the fatty acid metabolite oleoyl-CoA

We further explored the K_{2P} channel lipid sensitivity by testing the polyanionic lipid oleoyl-CoA, which represents a common cellular long-chain fatty acid metabolite. It is known to regulate ion channels (Rapedius et al., 2005; Ventura et al., 2005; Shumilina et al., 2006); however, it has not been investigated in K_{2P} channels so far. Upon application of 10 µM oleoyl-CoA, strong activation of TREK-1 (15 ± threefold) and weaker activation of TREK-2 (6 ± onefold) were observed (Fig. 2 A; Fig. S2, A and B; and

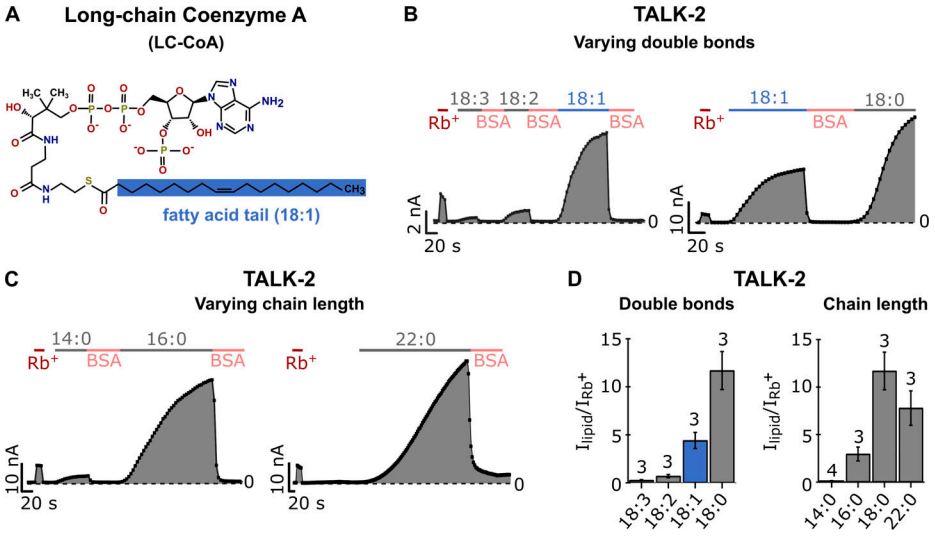

Figure 3. **Physicochemical properties of LC-CoA esters required for activation of TALK-2 K_{2P} channels. (A)** Chemical structure of LC-CoA (oleoyl-CoA; 18:1). The fatty acid tail is shaded blue. **(B)** Analyzed current traces at +80 mV of TALK-2 channels measured in voltage ramps between −80 and +80 mV in excised inside-out patches of *Xenopus* oocytes using control bath solution and in the presence of 3 µM of LC-CoA esters with varying number and position of double bonds (18:0, 18:1, 18:2, 18:3) in the fatty acid tail of the molecule or 5 mg ml^{-1} BSA. **(C)** Analyzed current traces at +80 mV of TALK-2 channels, measured as in B, using control bath solution and in the presence of 3 µM LC-CoA esters with varying chain length (14:0, 16:0, 18:0, 22:0) of the fatty acid tail. **(D)** Fold activation of TALK-2 channels by LC-CoA esters with varying double bonds or chain lengths, measured as in B and C and normalized to the respective Rb^+-activated current (red; B and C) at +80 mV. Data are summarized in Table S3. The average fold activation by Rb^+ ($I_{Rb}{}^+/I_{basal}$) of TALK-2 WT channels is 12 ± 3 (n = 20). Number of independent experiments is indicated above the bars. All data are presented as mean ± SEM.

Table S2). Notably, as seen with PIP_2 (Fig. 1 A; Fig. S1 C), TRAAK showed the highest lipid sensitivity within its subgroup, with oleoyl-CoA causing a 40 ± 16–fold current increase (Fig. 2, A and B). Furthermore, these activations were readily reversed upon extraction of oleoyl-CoA via the fatty acid binding protein BSA (Fig. 2 B; Fig. S2, A and B).

Similar to the PIP_2 responses, THIK-1 channels were strongly activated by oleoyl-CoA (29 ± 2-fold), whereas activation in THIK-2* was weaker (13.0 ± 0.4-fold; Fig. 2 A; Fig. S2, F and G).

In the TALK subfamily, TALK-2 stood out as oleoyl-CoA produced massive activation (94 ± 14-fold), while TALK-1 was only moderately activated (5 ± 1-fold; Fig. 2, A and B; Fig. S2 C).

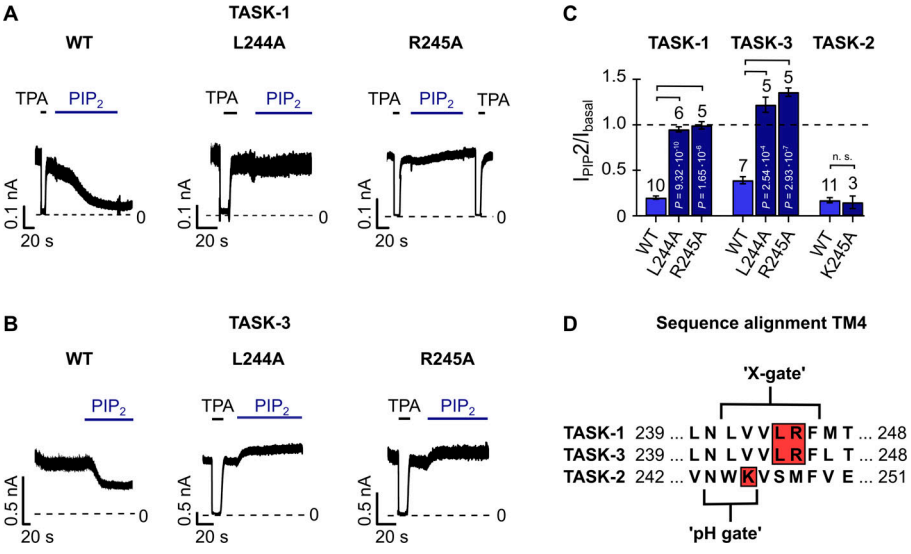

Figure 4. **Mutations within the lower gate (X-gate) prevent PIP_2 inhibition in TASK-1 and TASK-3 K_{2P} channels. (A and B)** Representative current traces of TASK-1 WT, L244A, and R245A mutant channels (A) and TASK-3 L244A and R245A mutant channels (B) measured at continuous +40 mV in excised inside-out patches of *Xenopus* oocytes using control bath solution and in the presence of 10 µM PIP_2 or 1 mM tetrapentylammonium chloride (TPA), showing that mutations disrupting the lower gate render the channels insensitive to PIP_2. **(C)** Fold change of TASK-1, TASK-3, and TASK-2 WT (light blue) and mutant (dark blue) currents analyzed at +40 mV in the presence of 10 µM PIP_2 measured as in A and B, Fig. 1 D (middle panel), or Fig. S1 J. Number of independent experiments is indicated above the bars. Data are summarized in Table S4. **(D)** Sequence alignment of TM4 of TASK-1, TASK-3, and TASK-2 K_{2P} channels. The lower X-gate in TASK-1 (TASK-3) and the region that forms the lower "pH gate" in TASK-2 are highlighted. Red boxes show the location of introduced mutations in the respective K_{2P} channel. All data are presented as mean ± SEM. Data in C are analyzed by unpaired Student's t test. P values are indicated. n. s., not significant.

In contrast, TASK-2 channels were inhibited by oleoyl-CoA (70 ± 7%; Fig. 2, A and C), again similar to the PIP_2 effects.

In the TASK subfamily, TASK-3 channels were inhibited by oleoyl-CoA (39 ± 5%) in contrast to TASK-1 channels that were rather slightly activated (Fig. 2 A; Fig. S2, D and E).

In the TWIK and TRESK subfamilies, both expressing members (i.e., TWIK-1* and TRESK) were markedly (~50 to ~75%) inhibited by oleoyl-CoA (Fig. 2, A and C; Fig. S2 H). As seen with all oleoyl-CoA effects reported here, application of BSA reversed the action of oleoyl-CoA.

In summary, with the exception of TASK-1, oleoyl-CoA application modulated the activity of all K_{2P} channels tested. Furthermore, the subfamily-specific response (i.e., activation versus inhibition) resembled the effects observed with PIP_2 in most cases. Exceptions to this rule were seen (1) for TASK-1, which was inhibited by PIP_2 but not by oleoyl-CoA, and (2) for TWIK-1* and TRESK, which were inhibited by oleoyl-CoA but lacked PIP_2 sensitivity.

Physicochemical requirements of LC-CoA activation in TALK-2 channels

Given the particularly high sensitivity of TALK-2 to oleoyl-CoA (Fig. 3 A), we chose this channel to explore the LC-CoA properties required for activation in more detail. Throughout the following measurements, we used Rb^+ activation in the beginning of each experiment for better quantification of the TALK-2–specific currents and BSA in the bath solution to accelerate the washout of oleoyl-CoA. We measured oleoyl-CoA activation for different concentrations ranging from 0.1 to 30 µM (Fig. S3, A and B), suggesting a half-maximal effect at a concentration of ~10 µM (Fig. S3 B). Notably, even concentrations as low as 100 nM already produced robust (>3-fold) TALK-2 channel activation (Fig. S3 A), consistent with the high maximal effect (i.e., >90-fold activation) at saturating concentrations (Fig. S3 B). Furthermore, the potency to activate TALK-2 channels negatively correlated with the number of LC-CoA double bonds present in fatty acids of 18–carbon atom chain length, with the saturated stearic acid being the most potent LC-CoA (Fig. 3, B and D). Moreover, for saturated fatty acids, the strongest activation was observed for stearyl-CoA, with shorter palmityl-CoA and longer docosanoyl-CoA being less potent (Fig. 3, C and D; and Table S3). These results (except the activity drop for docosanoyl-CoA) are qualitatively consistent with the notion that increasing acyl-chain length or reducing the number of double bonds is expected to promote LC-CoA membrane incorporation and thus would result in higher effective concentrations in the membrane from whence channel interactions are likely to occur. The drop of potency for docosanoyl-CoA (compared with stearyl-CoA) apparently conflicts with this simple concept, suggesting that possibly specific interactions of the fatty acid chain with the TALK-2 channel or changes in bilayer properties might also be important.

Location of the PIP_2 inhibition gate in TASK-1 and TASK-3

Here, we report the inhibition of TASK-2, TASK-1, TASK-3, TWIK-1*, and TRESK by the polyanionic lipids PIP_2 and oleoyl-CoA. This raises the question of the nature of the inhibition gate. Interestingly, TASK-1 and TASK-3 have previously been shown to be inhibited by DAG, and a region named the halothane response element in the distal TM4 segment was identified to be critical (Talley and Bayliss, 2002; Wilke et al., 2014). Moreover, in TASK-1, a gate at the halothane response element has recently been crystallographically identified and named the "X-gate" (Rödström et al., 2020). This X-gate forms a permeation-blocking pore constriction at the contact points of the TM4 helices, located halfway between the SF gate and the cytoplasmic pore entrance. Mutations within the lower X-gate (e.g., L244A and R245A; Fig. 4 D) have been shown to disturb channel closure, resulting in channels with a higher relative open probability (Rödström et al., 2020). Notably, we found that the mutations L244A and R245A completely abolished PIP_2 inhibition in TASK-1 and TASK-3 channels (Fig. 4, A–C; and Table S4), suggesting that PIP_2 induces closure of the X-gate similarly to DAG.

In the pH-sensitive TASK-2 channel, a lower gate at a location similar to the X-gate in TASK-1 has been identified recently in cryo-EM structures obtained at different pH (Li et al., 2020). This work identified a lysine residue (i.e., K245) within the lower gate as a pH-sensing residue and also as a critical component of the lower gate itself. However, mutation of this lysine to alanine (K245A) had no obvious effect on PIP_2 inhibition in TASK-2 (Fig. 4, C and D; Fig. S2 J). This suggests either that PIP_2 inhibition is mediated via a different gate (e.g., the SF) or that K245 is not critical for mediating PIP_2 inhibition via the lower gate in contrast to pH inhibition.

Discussion

Our comprehensive screen established K_{2P} channels as a family of K^+ channels highly sensitive to polyanionic membrane lipids such as PIP_2 and oleoyl-CoA. Furthermore, depending on the particular K_{2P} subfamily, polyanionic lipids either produced activation (TREK, TALK, and THIK subfamilies) or inhibition (TASK, TWIK, and TRESK subfamilies). The responses evoked in a particular subfamily produced by PIP_2 and oleoyl-CoA were similar, with three exceptions: (1) TWIK-1* and (2) TRESK were PIP_2 insensitive but were inhibited by oleoyl-CoA, and (3) TASK-1 was inhibited by PIP_2 but was oleoyl-CoA insensitive (Fig. 5 B).

Physiological implications of the PIP_2 regulation in K_{2P} channels

In the K_{ir} channel family, most if not all members are thought to require PIP_2 as a mandatory ligand to be functional (Huang et al., 1998; Logothetis et al., 2007; Fürst et al., 2014). For K_{2P} channels, not all members are activated by PIP_2, and thus PIP_2 can be considered a modulatory agent rather than a mandatory ligand. Accordingly, G protein–coupled receptor (GPCR; i.e., P_2Y_2) activation of PLC produced strong inhibition of TREK-1 activity (i.e., activity is no longer detectable) in HEK293 cells; however, subsequent activating stimuli (e.g., temperature increase) still produced robust activation (Fig. S1 K), indicating that PIP_2 is not strictly required for channel activity.

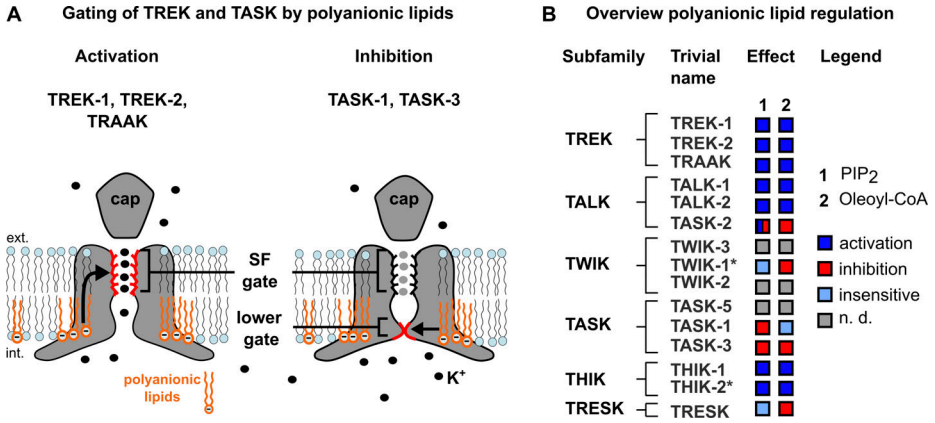

Figure 5. **Subtype-specific regulation of K_{2P} channels by polyanionic lipids. (A)** Gating cartoon depicting cross-sectional sketches of K_{2P} channels indicating the assumed locations of the gates regulated by polyanionic lipids (i.e., PIP_2 and oleoyl-CoA). In TREK-1, TREK-2, and TRAAK channels, the gate is located at the SF and opened by polyanionic lipids. In TASK-1 and TASK-3, the gate is located below the SF (lower gate/X-gate) and closed by polyanionic lipids. Note that the cartoon does not intend to indicate specific binding sites of the lipids. **(B)** Overview of the subtype-specific lipid effects in K_{2P} channels: dark blue box, activation; red box, inhibition; light blue box, insensitivity to the lipids with (1) PIP_2 and (2) oleoyl-CoA. The gray box indicates that the respective lipid effect was not determined (n. d.) to be caused by low functional channel expression.

Activation of TREK-1 channels by PIP_2 has been reported previously (Chemin et al, 2005, 2007; Soussia et al, 2018) as well as split responses with PIP_2 causing activation and inhibition (Chemin et al, 2007). Furthermore, in liposomes, PIP_2 caused inhibition of TREK-1 K^+ flux in the presence of PG, suggesting that PIP_2 might cause inhibition by competitive displacement of the strongly activatory lipids such as PG or PA (Cabanos et al., 2017). However, in our hands, inhibition of TREK-1/-2 channels was never observed in the *Xenopus* oocyte expression system. Resolving these discrepancies is difficult; however, possibly TREK-1/-2 might be liganded by strongly activatory lipids such as PA or PG to various degrees in cells, and then their competitive displacement by PIP_2 might result in channel inhibition (assuming PIP_2 is a less potent activator than the displaced lipid). Thus, the variable outcomes might be related to the actual lipid microenvironment or to the lipid ligandation situation at which PIP_2 is added to the TREK-1 channel. Also, the interaction of TREK-1 with PLD2 (producing PA) might differ in cells. Notably, TRAAK channels do not interact with PLD2 (Comoglio et al., 2014), and PIP_2 inhibition has not been reported. Here, we report that TRAAK channels exhibited the strongest PIP_2 response of all K_{2P} channels, with a >110-fold increase in channel activity. The physiological relevance of this PIP_2 regulation is currently unexplored but warrants further investigation in native preparations such as neurons that strongly express TRAAK channels (Brohawn et al., 2019; Kanda et al., 2019).

A notable finding of this work is the strong activation of THIK-1 channels by PIP_2 (Fig. 1, A and B). Despite its expression in many regions of the central nervous system, the specific role of THIK-1 channels is currently unknown, with the exception of microglial cells, where THIK-1 activation was shown to be involved in microglial immune surveillance and inflammatory cytokine release (Madry et al., 2018). Interestingly, PIP_2 production in microglia has been reported to play a key role in immune response signaling (Nguyen et al., 2017; Desale and Chinnathambi, 2021) and thus possibly involves PIP_2 activation of THIK-1.

We report here the inhibition of TASK-1 and TASK-3 channels by PIP_2. The involvement of the PIP_2 metabolism in the regulation of TASK-1 and TASK-3 has been intensively studied before, and it is currently assumed that GPCR-mediated release of DAG directly inhibits these channels, while the breakdown of PIP_2 appears not to be critical (Bista et al., 2015). Thus, the activation of TASK-1 and TASK-3 via membrane PIP_2 depletion (i.e., release of PIP_2 inhibition by, e.g., PLC activation) may not be of physiological relevance. However, inhibition of TASK-1 or TASK-3 via a local or global production of PIP_2 still could be a regulatory mechanism.

TASK-2 channels have previously been reported to be activated by the short-chain PIP_2 derivative dioctanoyl-PIP_2 (Niemeyer et al., 2017) which apparently contradicts the here reported inhibition of TASK-2 by application of the native (i.e., long-chain) $PI(4,5)P_2$. However, we found that the PIP_2 effect is clearly concentration dependent, with lower PIP_2 concentrations supporting TASK-2 activity consistent with the reactivation of rundown of TASK-2 channel currents. Longer PIP_2 applications as well as application on patches lacking current rundown produced robust and reliable inhibition. These findings might indicate that distinct regulatory PIP_2 sites exist in TASK-2 channels (i.e., a "higher" affinity activatory PIP_2 site and a "lower" affinity inhibitory PIP_2 site). Accordingly, at higher PIP_2 concentration, the inhibitory site dominates, causing inhibition in TASK-2 (as seen with TASK-1 and TASK-3), whereas lower PIP_2 concentration supports TASK-2 activity via the higher-affinity activatory site. However, these are rather speculative assumptions that clearly need further investigation.

It should also be pointed out that we provide only qualitative information on the effects of PIP_2 on the various channels and have not demonstrated direct channel PIP_2 interaction. Accordingly, we cannot rule out the possibility that PIP_2 might have affected the investigated K_{2P} channels also via indirect

mechanisms such as (1) changes in bilayer properties, (2) binding to accessory proteins, or (3) lipid metabolites (e.g., PA, DAG, arachidonic acid [AA]) produced by enzymes contained in an excised patch and initiated by the addition of PIP_2. For instance, PIP_2 is known to activate PLD2 (Bowling et al., 2020), which would indirectly activate TREK-1 through PA or PG production.

Physiological implications of the LC-CoA regulation in K_{2P} channels

LC-CoA represents ubiquitous cellular products of the fatty acid metabolism as fatty acids bound to CoA before they can be taken up by mitochondria for β-oxidation. Our study revealed the regulation of many K_{2P} channels by oleoyl-CoA. LC-CoA has previously been reported to modulate several members of the K_{ir} channel family (Larsson et al., 1996; Rohács et al., 2003; Rapedius et al., 2005; Shumilina et al., 2006; Tucker and Baukrowitz, 2008). K_{ATP} channels are thereby strongly activated, while most other K_{ir} channels are inhibited, likely because LC-CoA competes with PIP_2 for binding but lacks its activatory effect (competitive antagonism; Shumilina et al., 2006). Such competitive antagonism, however, is unlikely to cause the here reported inhibition in TASK-2, TASK-1, TASK-3, TWIK, and TRESK channels because these channels were not activated by PIP_2. However, in the PIP_2-activated channels (e.g., TREK-1), oleoyl-CoA likely interacts with the same sites as PIP_2 because the degree of oleoyl-CoA and PIP_2 activation is correlated in most K_{2P} channels.

The role of LC-CoA activation of K_{ATP} channels has been implicated in the mechanism of insulin secretion in pancreatic β cells, in fatty acid sensing in hypothalamic neurons, and in protection of cardiac myocytes under ischemic condition (Corkey et al., 2000; Liu et al., 2001; Tarasov et al., 2004; Le Foll et al., 2009; Rorsman and Ashcroft, 2018). These situations have in common that they cause an accumulation of LC-CoA in the cytoplasm, which potentially could also modulate the activity of the K_{2P} channels present in the respective tissues.

TALK-2 and TREK-1 channels are expressed in atrial as well as ventricular myocytes in the heart (Decher et al., 2001; Tan et al., 2004; Decher et al., 2017a). These channels are highly sensitive to LC-CoA as oleoyl-CoA caused a >15-fold activation (Fig. 2, A and B; Fig. S1, A and E). Therefore, activation of TALK-2 and TREK-1 channels under ischemic conditions may have cardioprotective effects in ventricular myocytes by shortening of action potential and concomitant reduction in Ca^{2+} loading (similar to K_{ATP} channels). However, this ischemic activation of TALK-2 and TREK-1 in the atrium causing action potential shortening could also potentially be arrhythmogenic.

It is noteworthy that TALK-2 (together with TALK-1) is expressed in pancreatic β-cells, but its physiological role is currently unknown (Duprat et al., 2005; Rorsman and Ashcroft, 2018; Graff et al., 2021). Thus, the accumulation of LC-CoA under conditions of hyperlipidemia and hyperglycemia could contribute to the known insulin secretion defects under these conditions because K^+ channel activation is expected to antagonize insulin secretion. Notably, the sensitivity of TALK-2 to oleoyl-CoA is higher than that of K_{ATP} channels because 10 nM oleoyl-CoA produced only little activation in K_{ATP} channels, whereas we report here robust activation for TALK-2 with this concentration (Larsson et al., 1996). Currently, rather little is known about the free concentrations of LC-CoA in cells, but calculations suggest a concentration in the range of 0.1 to 200 nM (Knudsen et al., 2000). Thus, our screening concentration of oleoyl-CoA (10 μM) is certainly very high, and more work is required to demonstrate the physiological relevance of the LC-CoA regulation in K_{2P} channels.

Structural insights into the mechanism of polyanionic lipid regulation

Based on crystallographic and functional data, it has been proposed that K_{2P} channels are regulated primarily via a highly dynamic SF gate located at the extracellular pore entrance (Bagriantsev et al., 2011; Piechotta et al., 2011; Bagriantsev et al., 2012; Schewe et al., 2016; Schewe et al., 2019) or via lipid binding below the SF blocking ion permeation (Brohawn et al., 2014). However, more recent structural studies revealed constriction sites in the ion permeation pathway below the SF in TASK-2 and TASK-1 channels (Li et al., 2020; Rödström et al., 2020). This raises the question of which of the two possible gating structures is relevant in the context of the here reported polyanionic lipid regulation in these channels (Fig. 5 A). In the TREK subfamily, the PIP_2/LC-CoA activation gate is likely the SF because lipid activation causes the transition of the voltage-dependent ion flux gating mode of the SF into the leak mode displaying a linear I-V (Fig. 2 B; Fig. 5 A; Fig. S1, A–C; Fig. S2, A and B; Schewe et al., 2016). However, THIK-1 channels display comparably little voltage gating, and thus the principal role of the SF gate is unresolved, and further experiments are required to determine the location of the PIP_2/LC-CoA activation gate. Likewise, the structural mechanism of TRESK channel inhibition by LC-CoA requires further investigation.

For TASK-1 and TASK-3 channels, our experiments suggest that inhibition by PIP_2 and LC-CoA involves the lower X-gate crystallographically identified in TASK-1 channels (and assumed for TASK-3 channels), as the published mutations within this region also abolished PIP_2 inhibition in both channels. However, the location of the PIP_2/LC-CoA binding sites, as well as the possible overlap with the still unknown inhibitory DAG binding site, will require further investigation. In TASK-2 channels, a lower gate mediating pH inhibition was recently identified in cryo-EM structures at a location similar to the X-gate in TASK-1 (Li et al., 2020). Although its involvement in PIP_2/LC-CoA inhibition seems reasonable, mutation of a critical residue at the intracellular pH gate did not affect PIP_2 inhibition (Fig. 4 C and Fig. S1 J). Thus, additional studies are required to clarify the structural mechanisms of polyanionic lipid inhibition in TASK-2.

Conclusions

This work establishes common polyanionic cellular lipids such as PIP_2 and LC-CoA as regulators of channel activity for all 12 functionally expressing mammalian K_{2P} channels. We provide first insights into the location of the PIP_2/LC-CoA inhibition gate in TASK-1 and TASK-3, but substantially more work is required

to disclose the lipid binding sites in the various K_{2P} channels as well as the structural mechanism underlying the polyanionic lipid regulation. Finally, investigation of the relevant signal transduction pathways in native preparations is required to demonstrate the physiological relevance of linking K_{2P} channel activity to the complex metabolisms of phosphoinositides and fatty acids in the various tissues and cell types expressing K_{2P} channels.

Data availability

The data supporting the findings of this study are available from the corresponding authors upon reasonable request.

Acknowledgments

Crina M. Nimigean served as editor.

We thank members of our laboratory for helpful comments on the manuscript and technical support of the project.

These studies were supported by funding from the Deutsche Forschungsgemeinschaft to M. Schewe and T. Baukrowitz as part of the Research Unit FOR2518, DynIon.

The authors declare no competing financial interest.

Author contributions: M. Schewe and T. Baukrowitz conceived and supervised the project; E.B. Riel, B.C. Jürs, S. Cordeiro, and M. Schewe performed all patch-clamp experiments and analyzed the data; M. Musinszki created and supervised the generation of mutant channels; E.B. Riel prepared all figures; E.B. Riel, M. Schewe, and T. Baukrowitz wrote the original manuscript draft and reviewed/edited the draft; M. Schewe and T. Baukrowitz obtained funding.

Submitted: 2 July 2021
Accepted: 1 December 2021

References

Alloui, A., K. Zimmermann, J. Mamet, F. Duprat, J. Noël, J. Chemin, N. Guy, N. Blondeau, N. Voilley, C. Rubat-Coudert, et al. 2006. TREK-1, a K^+ channel involved in polymodal pain perception. *EMBO J.* 25:2368–2376. https://doi.org/10.1038/sj.emboj.7601116

Andres-Enguix, I., L. Shang, P.J. Stansfeld, J.M. Morahan, M.S. Sansom, R.G. Lafrenière, B. Roy, L.R. Griffiths, G.A. Rouleau, G.C. Ebers, et al. 2012. Functional analysis of missense variants in the TRESK (KCNK18) K channel. *Sci. Rep.* 2:237. https://doi.org/10.1038/srep00237

Antigny, F., A. Hautefort, J. Meloche, M. Belacel-Ouari, B. Manoury, C. Rucker-Martin, C. Péchoux, F. Potus, V. Nadeau, E. Tremblay, et al. 2016. Potassium channel subfamily K member 3 (KCNK3) contributes to the development of pulmonary arterial hypertension. *Circulation.* 133: 1371–1385. https://doi.org/10.1161/CIRCULATIONAHA.115.020951

Ashmole, I., P.A. Goodwin, and P.R. Stanfield. 2001. TASK-5, a novel member of the tandem pore K^+ channel family. *Pflugers Arch.* 442:828–833. https://doi.org/10.1007/s004240100620

Bagriantsev, S.N., R. Peyronnet, K.A. Clark, E. Honoré, and D.L. Minor Jr. 2011. Multiple modalities converge on a common gate to control K2P channel function. *EMBO J.* 30:3594–3606. https://doi.org/10.1038/emboj.2011.230

Bagriantsev, S.N., K.A. Clark, and D.L. Minor, Jr.. 2012. Metabolic and thermal stimuli control $K_{2P}2.1$ (TREK-1) through modular sensory and gating domains. *EMBO J.* 31:3297–3308. https://doi.org/10.1038/emboj.2012.171

Bandulik, S., P. Tauber, E. Lalli, J. Barhanin, and R. Warth. 2015. Two-pore domain potassium channels in the adrenal cortex. *Pflugers Arch.* 467: 1027–1042. https://doi.org/10.1007/s00424-014-1628-6

Bayliss, D.A., E.M. Talley, J.E. Sirois, and Q. Lei. 2001. TASK-1 is a highly modulated pH-sensitive 'leak' K^+ channel expressed in brainstem respiratory neurons. *Respir. Physiol.* 129:159–174. https://doi.org/10.1016/S0034-5687(01)00288-2

Bichet, D., S. Blin, S. Feliciangeli, F.C. Chatelain, N. Bobak, and F. Lesage. 2015. Silent but not dumb: how cellular trafficking and pore gating modulate expression of TWIK1 and THIK2. *Pflugers Arch.* 467:1121–1131. https://doi.org/10.1007/s00424-014-1631-y

Bista, P., M. Pawlowski, M. Cerina, P. Ehling, M. Leist, P. Meuth, A. Aissaoui, M. Borsotto, C. Heurteaux, N. Decher, et al. 2015. Differential phospholipase C-dependent modulation of TASK and TREK two-pore domain K^+ channels in rat thalamocortical relay neurons. *J. Physiol.* 593: 127–144. https://doi.org/10.1113/jphysiol.2014.276527

Bowling, F.Z., C.M. Salazar, J.A. Bell, T.S. Huq, M.A. Frohman, and M.V. Airola. 2020. Crystal structure of human PLD1 provides insight into activation by $PI(4,5)P_2$ and RhoA. *Nat. Chem. Biol.* 16:400–407. https://doi.org/10.1038/s41589-020-0499-8

Bränström, R., I.B. Leibiger, B. Leibiger, B.E. Corkey, P.O. Berggren, and O. Larsson. 1998. Long chain coenzyme A esters activate the pore-forming subunit (Kir6. 2) of the ATP-regulated potassium channel. *J. Biol. Chem.* 273:31395–31400. https://doi.org/10.1074/jbc.273.47.31395

Brohawn, S.G., E.B. Campbell, and R. MacKinnon. 2014. Physical mechanism for gating and mechanosensitivity of the human TRAAK K^+ channel. *Nature.* 516:126–130. https://doi.org/10.1038/nature14013

Brohawn, S.G., W. Wang, A. Handler, E.B. Campbell, J.R. Schwarz, and R. MacKinnon. 2019. The mechanosensitive ion channel TRAAK is localized to the mammalian node of Ranvier. *eLife.* 8:e50403. https://doi.org/10.7554/eLife.50403

Cabanos, C., M. Wang, X. Han, and S.B. Hansen. 2017. A soluble fluorescent binding assay reveals PIP_2 antagonism of TREK-1 channels. *Cell Rep.* 20: 1287–1294. https://doi.org/10.1016/j.celrep.2017.07.034

Chemin, J., A.J. Patel, F. Duprat, I. Lauritzen, M. Lazdunski, and E. Honoré. 2005. A phospholipid sensor controls mechanogating of the K^+ channel TREK-1. *EMBO J.* 24:44–53. https://doi.org/10.1038/sj.emboj.7600494

Chemin, J., A.J. Patel, F. Duprat, F. Sachs, M. Lazdunski, and E. Honore. 2007. Up- and down-regulation of the mechano-gated K_{2P} channel TREK-1 by PIP_2 and other membrane phospholipids. *Pflugers Arch.* 455:97–103. https://doi.org/10.1007/s00424-007-0250-2

Cheng, W.W.L., N. D'Avanzo, D.A. Doyle, and C.G. Nichols. 2011. Dual-mode phospholipid regulation of human inward rectifying potassium channels. *Biophys. J.* 100:620–628. https://doi.org/10.1016/j.bpj.2010.12.3724

Comoglio, Y., J. Levitz, M.A. Kienzler, F. Lesage, E.Y. Isacoff, and G. Sandoz. 2014. Phospholipase D2 specifically regulates TREK potassium channels via direct interaction and local production of phosphatidic acid. *Proc. Natl. Acad. Sci. USA.* 111:13547–13552. https://doi.org/10.1073/pnas.1407160111

Corkey, B.E., J.T. Deeney, G.C. Yaney, K. Tornheim, and M. Prentki. 2000. The role of long-chain fatty acyl-CoA esters in β-cell signal transduction. *J. Nutr.* 130(2S, Suppl):299S–304S. https://doi.org/10.1093/jn/130.2.299S

Czirják, G., Z.E. Tóth, and P. Enyedi. 2004. The two-pore domain K^+ channel, TRESK, is activated by the cytoplasmic calcium signal through calcineurin. *J. Biol. Chem.* 279:18550–18558. https://doi.org/10.1074/jbc.M312229200

Davies, L.A., C. Hu, N.A. Guagliardo, N. Sen, X. Chen, E.M. Talley, R.M. Carey, D.A. Bayliss, and P.Q. Barrett. 2008. TASK channel deletion in mice causes primary hyperaldosteronism. *Proc. Natl. Acad. Sci. USA.* 105: 2203–2208. https://doi.org/10.1073/pnas.0712000105

Decher, N., M. Maier, W. Dittrich, J. Gassenhuber, A. Brüggemann, A.E. Busch, and K. Steinmeyer. 2001. Characterization of TASK-4, a novel member of the pH-sensitive, two-pore domain potassium channel family. *FEBS Lett.* 492:84–89. https://doi.org/10.1016/S0014-5793(01)02222-0

Decher, N., A.K. Kiper, and S. Rinné. 2017a. Stretch-activated potassium currents in the heart: Focus on TREK-1 and arrhythmias. *Prog. Biophys. Mol. Biol.* 130(Pt B):223–232. https://doi.org/10.1016/j.pbiomolbio.2017.05.005

Decher, N., B. Ortiz-Bonnin, C. Friedrich, M. Schewe, A.K. Kiper, S. Rinné, G. Seemann, R. Peyronnet, S. Zumhagen, D. Bustos, et al. 2017b. Sodium permeable and "hypersensitive" TREK-1 channels cause ventricular tachycardia. *EMBO Mol. Med.* 9:403–414. https://doi.org/10.15252/emmm.201606690

Desale, S.E., and S. Chinnathambi. 2021. Phosphoinositides signaling modulates microglial actin remodeling and phagocytosis in Alzheimer's disease. *Cell Commun. Signal.* 19:28. https://doi.org/10.1186/s12964-021-00715-0

Duprat, F., C. Girard, G. Jarretou, and M. Lazdunski. 2005. Pancreatic two P domain K^+ channels TALK-1 and TALK-2 are activated by nitric oxide

and reactive oxygen species. *J. Physiol.* 562:235–244. https://doi.org/10.1113/jphysiol.2004.071266

Effertz, T., L. Becker, A.W. Peng, and A.J. Ricci. 2017. Phosphoinositol-4,5-bisphosphate regulates auditory hair-cell mechanotransduction-channel pore properties and fast adaptation. *J. Neurosci.* 37:11632–11646. https://doi.org/10.1523/JNEUROSCI.1351-17.2017

Enyedi, P., and G. Czirják. 2010. Molecular background of leak K^+ currents: two-pore domain potassium channels. *Physiol. Rev.* 90:559–605. https://doi.org/10.1152/physrev.00029.2009

Feliciangeli, S., S. Bendahhou, G. Sandoz, P. Gounon, M. Reichold, R. Warth, M. Lazdunski, J. Barhanin, and F. Lesage. 2007. Does sumoylation control K2P1/TWIK1 background K^+ channels? *Cell.* 130:563–569. https://doi.org/10.1016/j.cell.2007.06.012

Feliciangeli, S., M.P. Tardy, G. Sandoz, F.C. Chatelain, R. Warth, J. Barhanin, S. Bendahhou, and F. Lesage. 2010. Potassium channel silencing by constitutive endocytosis and intracellular sequestration. *J. Biol. Chem.* 285:4798–4805. https://doi.org/10.1074/jbc.M109.078535

Fürst, O., B. Mondou, and N. D'Avanzo. 2014. Phosphoinositide regulation of inward rectifier potassium (Kir) channels. *Front. Physiol.* 4:404. https://doi.org/10.3389/fphys.2013.00404

Gamper, N., and M.S. Shapiro. 2007. Regulation of ion transport proteins by membrane phosphoinositides. *Nat. Rev. Neurosci.* 8:921–934. https://doi.org/10.1038/nrn2257

Giblin, J.P., I. Etayo, A. Castellanos, A. Andres-Bilbe, and X. Gasull. 2019. Anionic phospholipids bind to and modulate the activity of human TRESK background K^+ channel. *Mol. Neurobiol.* 56:2524–2541. https://doi.org/10.1007/s12035-018-1244-0

Graff, S.M., S.R. Johnson, P.J. Leo, P.K. Dadi, M.T. Dickerson, A.Y. Nakhe, A.M. McInerney-Leo, M. Marshall, K.E. Zaborska, C.M. Schaub, et al. 2021. A KCNK16 mutation causing TALK-1 gain of function is associated with maturity-onset diabetes of the young. *JCI Insight.* 6:e138057. https://doi.org/10.1172/jci.insight.138057

Hansen, S.B., X. Tao, and R. MacKinnon. 2011. Structural basis of PIP2 activation of the classical inward rectifier K^+ channel Kir2.2. *Nature.* 477:495–498. https://doi.org/10.1038/nature10370

Heurteaux, C., G. Lucas, N. Guy, M. El Yacoubi, S. Thümmler, X.D. Peng, F. Noble, N. Blondeau, C. Widmann, M. Borsotto, et al. 2006. Deletion of the background potassium channel TREK-1 results in a depression-resistant phenotype. *Nat. Neurosci.* 9:1134–1141. https://doi.org/10.1038/nn1749

Hilgemann, D.W., S. Feng, and C. Nasuhoglu. 2001. The complex and intriguing lives of PIP2 with ion channels and transporters. *Sci. STKE.* 2001:re19. https://doi.org/10.1126/stke.2001.111.re19

Hirono, M., C.S. Denis, G.P. Richardson, and P.G. Gillespie. 2004. Hair cells require phosphatidylinositol 4,5-bisphosphate for mechanical transduction and adaptation. *Neuron.* 44:309–320. https://doi.org/10.1016/j.neuron.2004.09.020

Honoré, E., F. Maingret, M. Lazdunski, and A.J. Patel. 2002. An intracellular proton sensor commands lipid- and mechano-gating of the K^+ channel TREK-1. *EMBO J.* 21:2968–2976. https://doi.org/10.1093/emboj/cdf288

Huang, C.L., S. Feng, and D.W. Hilgemann. 1998. Direct activation of inward rectifier potassium channels by PIP2 and its stabilization by Gbeta-gamma. *Nature.* 391:803–806. https://doi.org/10.1038/35882

Kanda, H., J. Ling, S. Tonomura, K. Noguchi, S. Matalon, and J.G. Gu. 2019. TREK-1 and TRAAK are principal K^+ channels at the nodes of Ranvier for rapid action potential conduction on mammalian myelinated afferent nerves. *Neuron.* 104:960–971.e7. https://doi.org/10.1016/j.neuron.2019.08.042

Knudsen, J., T.B. Neergaard, B. Gaigg, M.V. Jensen, and J.K. Hansen. 2000. Role of acyl-CoA binding protein in acyl-CoA metabolism and acyl-CoA-mediated cell signaling. *J. Nutr.* 130(2S, Suppl):294S–298S. https://doi.org/10.1093/jn/130.2.294S

Kruse, M., G.R. Hammond, and B. Hille. 2012. Regulation of voltage-gated potassium channels by PI(4,5)P2. *J. Gen. Physiol.* 140:189–205. https://doi.org/10.1085/jgp.201210806

Lafrenière, R.G., M.Z. Cader, J.F. Poulin, I. Andres-Enguix, M. Simoneau, N. Gupta, K. Boisvert, F. Lafrenière, S. McLaughlan, M.P. Dubé, et al. 2010. A dominant-negative mutation in the TRESK potassium channel is linked to familial migraine with aura. *Nat. Med.* 16:1157–1160. https://doi.org/10.1038/nm.2216

Larsson, O., J.T. Deeney, R. Bränström, P.O. Berggren, and B.E. Corkey. 1996. Activation of the ATP-sensitive K^+ channel by long chain acyl-CoA. A role in modulation of pancreatic β-cell glucose sensitivity. *J. Biol. Chem.* 271:10623–10626. https://doi.org/10.1074/jbc.271.18.10623

Le Foll, C., B.G. Irani, C. Magnan, A.A. Dunn-Meynell, and B.E. Levin. 2009. Characteristics and mechanisms of hypothalamic neuronal fatty acid sensing. *Am. J. Physiol. Regul. Integr. Comp. Physiol.* 297:R655–R664. https://doi.org/10.1152/ajpregu.00223.2009

Li, B., R.A. Rietmeijer, and S.G. Brohawn. 2020. Structural basis for pH gating of the two-pore domain K^+ channel TASK2. *Nature.* 586:457–462. https://doi.org/10.1038/s41586-020-2770-2

Liang, B., M. Soka, A.H. Christensen, M.S. Olesen, A.P. Larsen, F.K. Knop, F. Wang, J.B. Nielsen, M.N. Andersen, D. Humphreys, et al. 2014. Genetic variation in the two-pore domain potassium channel, TASK-1, may contribute to an atrial substrate for arrhythmogenesis. *J. Mol. Cell. Cardiol.* 67:69–76. https://doi.org/10.1016/j.yjmcc.2013.12.014

Liu, G.X., P.J. Hanley, J. Ray, and J. Daut. 2001. Long-chain acyl-coenzyme A esters and fatty acids directly link metabolism to K_{ATP} channels in the heart. *Circ. Res.* 88:918–924. https://doi.org/10.1161/hh0901.089881

Logothetis, D.E., T. Jin, D. Lupyan, and A. Rosenhouse-Dantsker. 2007. Phosphoinositide-mediated gating of inwardly rectifying K^+ channels. *Pflugers Arch.* 455:83–95. https://doi.org/10.1007/s00424-007-0276-5

Lopes, C.M., T. Rohács, G. Czirják, T. Balla, P. Enyedi, and D.E. Logothetis. 2005. PIP2 hydrolysis underlies agonist-induced inhibition and regulates voltage gating of two-pore domain K^+ channels. *J. Physiol.* 564:117–129. https://doi.org/10.1113/jphysiol.2004.081935

Ma, L., D. Roman-Campos, E.D. Austin, M. Eyries, K.S. Sampson, F. Soubrier, M. Germain, D.A. Trégouët, A. Borczuk, E.B. Rosenzweig, et al. 2013. A novel channelopathy in pulmonary arterial hypertension. *N. Engl. J. Med.* 369:351–361. https://doi.org/10.1056/NEJMoa1211097

Madry, C., V. Kyrargyri, I.L. Arancibia-Cárcamo, R. Jolivet, S. Kohsaka, R.M. Bryan, and D. Attwell. 2018. Microglial ramification, surveillance, and interleukin-1β release are regulated by the two-pore domain K^+ channel THIK-1. *Neuron.* 97:299–312.e6. https://doi.org/10.1016/j.neuron.2017.12.002

Maingret, F., A.J. Patel, F. Lesage, M. Lazdunski, and E. Honoré. 1999. Mechano- or acid stimulation, two interactive modes of activation of the TREK-1 potassium channel. *J. Biol. Chem.* 274:26691–26696. https://doi.org/10.1074/jbc.274.38.26691

Maingret, F., I. Lauritzen, A.J. Patel, C. Heurteaux, R. Reyes, F. Lesage, M. Lazdunski, and E. Honoré. 2000a. TREK-1 is a heat-activated background K^+ channel. *EMBO J.* 19:2483–2491. https://doi.org/10.1093/emboj/19.11.2483

Maingret, F., A.J. Patel, F. Lesage, M. Lazdunski, and E. Honoré. 2000b. Lysophospholipids open the two-pore domain mechano-gated K^+ channels TREK-1 and TRAAK. *J. Biol. Chem.* 275:10128–10133. https://doi.org/10.1074/jbc.275.14.10128

Maingret, F., E. Honoré, M. Lazdunski, and A.J. Patel. 2002. Molecular basis of the voltage-dependent gating of TREK-1, a mechano-sensitive K^+ channel. *Biochem. Biophys. Res. Commun.* 292:339–346. https://doi.org/10.1006/bbrc.2002.6674

Morton, M.J., A.D. O'Connell, A. Sivaprasadarao, and M. Hunter. 2003. Determinants of pH sensing in the two-pore domain K^+ channels TASK-1 and -2. *Pflugers Arch.* 445:577–583. https://doi.org/10.1007/s00424-002-0901-2

Nematian-Ardestani, E., F. Abd-Wahab, F.C. Chatelain, H. Sun, M. Schewe, T. Baukrowitz, and S.J. Tucker. 2020. Selectivity filter instability dominates the low intrinsic activity of the TWIK-1 K2P K^+ channel. *J. Biol. Chem.* 295:610–618. https://doi.org/10.1074/jbc.RA119.010612

Nguyen, T.T.N., E. Seo, J. Choi, O.T.T. Le, J.Y. Kim, I. Jou, and S.Y. Lee. 2017. Phosphatidylinositol 4-phosphate 5-kinase α contributes to Toll-like receptor 2-mediated immune responses in microglial cells stimulated with lipoteichoic acid. *Cell. Signal.* 38:159–170. https://doi.org/10.1016/j.cellsig.2017.07.009

Niemeyer, M.I., L.P. Cid, G. Peña-Münzenmayer, and F.V. Sepúlveda. 2010. Separate gating mechanisms mediate the regulation of K2P potassium channel TASK-2 by intra- and extracellular pH. *J. Biol. Chem.* 285:16467–16475. https://doi.org/10.1074/jbc.M110.107060

Niemeyer, M.I., L.P. Cid, M. Paulais, J. Teulon, and F.V. Sepúlveda. 2017. Phosphatidylinositol (4,5)-bisphosphate dynamically regulates the K_{2P} background K^+ channel TASK-2. *Sci. Rep.* 7:45407. https://doi.org/10.1038/srep45407

Niu, Y., X. Tao, K.K. Touhara, and R. MacKinnon. 2020. Cryo-EM analysis of PIP_2 regulation in mammalian GIRK channels. *eLife.* 9:e60552. https://doi.org/10.7554/eLife.60552

Oliver, D., C.C. Lien, M. Soom, T. Baukrowitz, P. Jonas, and B. Fakler. 2004. Functional conversion between A-type and delayed rectifier K^+ channels by membrane lipids. *Science.* 304:265–270. https://doi.org/10.1126/science.1094113

Olschewski, A., Y. Li, B. Tang, J. Hanze, B. Eul, R.M. Bohle, J. Wilhelm, R.E. Morty, M.E. Brau, E.K. Weir, et al. 2006. Impact of TASK-1 in human pulmonary artery smooth muscle cells. *Circ. Res.* 98:1072–1080. https://doi.org/10.1161/01.RES.0000219677.12988.e9

Pian, P., A. Bucchi, R.B. Robinson, and S.A. Siegelbaum. 2006. Regulation of gating and rundown of HCN hyperpolarization-activated channels by exogenous and endogenous PIP2. *J. Gen. Physiol.* 128:593–604. https://doi.org/10.1085/jgp.200609648

Piechotta, P.L., M. Rapedius, P.J. Stansfeld, M.K. Bollepalli, G. Ehrlich, I. Andres-Enguix, H. Fritzenschaft, N. Decher, M.S. Sansom, S.J. Tucker, and T. Baukrowitz. 2011. The pore structure and gating mechanism of K2P channels. *EMBO J.* 30:3607–3619. https://doi.org/10.1038/emboj.2011.268

Plant, L.D., S. Rajan, and S.A. Goldstein. 2005. K2P channels and their protein partners. *Curr. Opin. Neurobiol.* 15:326–333. https://doi.org/10.1016/j.conb.2005.05.008

Plant, L.D., I.S. Dementieva, A. Kollewe, S. Olikara, J.D. Marks, and S.A. Goldstein. 2010. One SUMO is sufficient to silence the dimeric potassium channel K2P1. *Proc. Natl. Acad. Sci. USA.* 107:10743–10748. https://doi.org/10.1073/pnas.1004712107

Qin, F. 2007. Regulation of TRP ion channels by phosphatidylinositol-4,5-bisphosphate. *Handb. Exp. Pharmacol.* 179:509–525. https://doi.org/10.1007/978-3-540-34891-7_30

Rajan, S., E. Wischmeyer, G. Xin Liu, R. Preisig-Müller, J. Daut, A. Karschin, and C. Derst. 2000. TASK-3, a novel tandem pore domain acid-sensitive K^+ channel. An extracellular histiding as pH sensor. *J. Biol. Chem.* 275:16650–16657. https://doi.org/10.1074/jbc.M000030200

Rajan, S., L.D. Plant, M.L. Rabin, M.H. Butler, and S.A. Goldstein. 2005. Sumoylation silences the plasma membrane leak K^+ channel K2P1. *Cell.* 121:37–47. https://doi.org/10.1016/j.cell.2005.01.019

Rapedius, M., M. Soom, E. Shumilina, D. Schulze, R. Schönherr, C. Kirsch, F. Lang, S.J. Tucker, and T. Baukrowitz. 2005. Long chain CoA esters as competitive antagonists of phosphatidylinositol 4,5-bisphosphate activation in Kir channels. *J. Biol. Chem.* 280:30760–30767. https://doi.org/10.1074/jbc.M503503200

Rodriguez, N., M.Y. Amarouch, J. Montnach, J. Piron, A.J. Labro, F. Charpentier, J. Mérot, I. Baró, and G. Loussouarn. 2010. Phosphatidylinositol-4,5-bisphosphate (PIP_2) stabilizes the open pore conformation of the Kv11.1 (hERG) channel. *Biophys. J.* 99:1110–1118. https://doi.org/10.1016/j.bpj.2010.06.013

Rödström, K.E.J., A.K. Kiper, W. Zhang, S. Rinné, A.C.W. Pike, M. Goldstein, L.J. Conrad, M. Delbeck, M.G. Hahn, H. Meier, et al. 2020. A lower X-gate in TASK channels traps inhibitors within the vestibule. *Nature.* 582:443–447. https://doi.org/10.1038/s41586-020-2250-8

Rohács, T., C.M. Lopes, T. Jin, P.P. Ramdya, Z. Molnár, and D.E. Logothetis. 2003. Specificity of activation by phosphoinositides determines lipid regulation of Kir channels. *Proc. Natl. Acad. Sci. USA.* 100:745–750. https://doi.org/10.1073/pnas.0236364100

Rorsman, P., and F.M. Ashcroft. 2018. Pancreatic β-cell electrical activity and insulin secretion: of mice and men. *Physiol. Rev.* 98:117–214. https://doi.org/10.1152/physrev.00008.2017

Royal, P., A. Andres-Bilbe, P. Ávalos Prado, C. Verkest, B. Wdziekonski, S. Schaub, A. Baron, F. Lesage, X. Gasull, J. Levitz, and G. Sandoz. 2019. Migraine-associated TRESK mutations increase neuronal excitability through alternative translation initiation and inhibition of TREK. *Neuron.* 101:232–245.e6. https://doi.org/10.1016/j.neuron.2018.11.039

Sandoz, G., S. Thümmler, F. Duprat, S. Feliciangeli, J. Vinh, P. Escoubas, N. Guy, M. Lazdunski, and F. Lesage. 2006. AKAP150, a switch to convert mechano-, pH- and arachidonic acid-sensitive TREK K^+ channels into open leak channels. *EMBO J.* 25:5864–5872. https://doi.org/10.1038/sj.emboj.7601437

Schewe, M., E. Nematian-Ardestani, H. Sun, M. Musinszki, S. Cordeiro, G. Bucci, B.L. de Groot, S.J. Tucker, M. Rapedius, and T. Baukrowitz. 2016. A non-canonical voltage-sensing mechanism controls gating in K2P K^+ channels. *Cell.* 164:937–949. https://doi.org/10.1016/j.cell.2016.02.002

Schewe, M., H. Sun, Ü. Mert, A. Mackenzie, A.C.W. Pike, F. Schulz, C. Constantin, K.S. Vowinkel, L.J. Conrad, A.K. Kiper, et al. 2019. A pharmacological master key mechanism that unlocks the selectivity filter gate in K^+ channels. *Science.* 363:875–880. https://doi.org/10.1126/science.aav0569

Schrecke, S., Y. Zhu, J.W. McCabe, M. Bartz, C. Packianathan, M. Zhao, M. Zhou, D. Russell, and A. Laganowsky. 2021. Selective regulation of human TRAAK channels by biologically active phospholipids. *Nat. Chem. Biol.* 17:89–95. https://doi.org/10.1038/s41589-020-00659-5

Schulze, D., M. Rapedius, T. Krauter, and T. Baukrowitz. 2003. Long-chain acyl-CoA esters and phosphatidylinositol phosphates modulate ATP inhibition of KATP channels by the same mechanism. *J. Physiol.* 552:357–367. https://doi.org/10.1113/jphysiol.2003.047035

Shumilina, E., N. Klöcker, G. Korniychuk, M. Rapedius, F. Lang, and T. Baukrowitz. 2006. Cytoplasmic accumulation of long-chain coenzyme A esters activates KATP and inhibits Kir2.1 channels. *J. Physiol.* 575:433–442. https://doi.org/10.1113/jphysiol.2006.111161

Soussia, I.B., F.S. Choveau, S. Blin, E.J. Kim, S. Feliciangeli, F.C. Chatelain, D. Kang, D. Bichet, and F. Lesage. 2018. Antagonistic effect of a cytoplasmic domain on the basal activity of polymodal potassium channels. *Front. Mol. Neurosci.* 11:301. https://doi.org/10.3389/fnmol.2018.00301

Suh, B.C., and B. Hille. 2005. Regulation of ion channels by phosphatidylinositol 4,5-bisphosphate. *Curr. Opin. Neurobiol.* 15:370–378. https://doi.org/10.1016/j.conb.2005.05.005

Suh, B.C., and B. Hille. 2008. PIP2 is a necessary cofactor for ion channel function: how and why? *Annu. Rev. Biophys.* 37:175–195. https://doi.org/10.1146/annurev.biophys.37.032807.125859

Sun, J., and R. MacKinnon. 2020. Structural basis of human KCNQ1 modulation and gating. *Cell.* 180:340–347.e9. https://doi.org/10.1016/j.cell.2019.12.003

Talley, E.M., and D.A. Bayliss. 2002. Modulation of TASK-1 (Kcnk3) and TASK-3 (Kcnk9) potassium channels: volatile anesthetics and neurotransmitters share a molecular site of action. *J. Biol. Chem.* 277:17733–17742. https://doi.org/10.1074/jbc.M200502200

Tan, J.H., W. Liu, and D.A. Saint. 2004. Differential expression of the mechanosensitive potassium channel TREK-1 in epicardial and endocardial myocytes in rat ventricle. *Exp. Physiol.* 89:237–242. https://doi.org/10.1113/expphysiol.2003.027052

Tarasov, A., J. Dusonchet, and F. Ashcroft. 2004. Metabolic regulation of the pancreatic β-cell ATP-sensitive K^+ channel: a pas de deux. *Diabetes.* 53(Suppl 3):S113–S122. https://doi.org/10.2337/diabetes.53.suppl_3.S113

Taylor, K.C., and C.R. Sanders. 2017. Regulation of KCNQ/Kv7 family voltage-gated K^+ channels by lipids. *Biochim. Biophys. Acta Biomembr.* 1859:586–597. https://doi.org/10.1016/j.bbamem.2016.10.023

Tucker, S.J., and T. Baukrowitz. 2008. How highly charged anionic lipids bind and regulate ion channels. *J. Gen. Physiol.* 131:431–438. https://doi.org/10.1085/jgp.200709936

Vaithianathan, T., A. Bukiya, J. Liu, P. Liu, M. Asuncion-Chin, Z. Fan, and A. Dopico. 2008. Direct regulation of BK channels by phosphatidylinositol 4,5-bisphosphate as a novel signaling pathway. *J. Gen. Physiol.* 132:13–28. https://doi.org/10.1085/jgp.200709913

Ventura, F.V., J. Ruiter, L. Ijlst, I.T. de Almeida, and R.J. Wanders. 2005. Differential inhibitory effect of long-chain acyl-CoA esters on succinate and glutamate transport into rat liver mitochondria and its possible implications for long-chain fatty acid oxidation defects. *Mol. Genet. Metab.* 86:344–352. https://doi.org/10.1016/j.ymgme.2005.07.030

Wilke, B.U., M. Lindner, L. Greifenberg, A. Albus, Y. Kronimus, M. Bünemann, M.G. Leitner, and D. Oliver. 2014. Diacylglycerol mediates regulation of TASK potassium channels by Gq-coupled receptors. *Nat. Commun.* 5:5540. https://doi.org/10.1038/ncomms6540

Ying, S.W., G.R. Tibbs, A. Picollo, S.Y. Abbas, R.L. Sanford, A. Accardi, F. Hofmann, A. Ludwig, and P.A. Goldstein. 2011. PIP2-mediated HCN3 channel gating is crucial for rhythmic burst firing in thalamic intergeniculate leaflet neurons. *J. Neurosci.* 31:10412–10423. https://doi.org/10.1523/JNEUROSCI.0021-11.2011

Yu, Y., C.R. Carter, N. Youssef, J.R. Dyck, and P.E. Light. 2014. Intracellular long-chain acyl CoAs activate TRPV1 channels. *PLoS One.* 9:e96597. https://doi.org/10.1371/journal.pone.0096597

Zaydman, M.A., and J. Cui. 2014. PIP2 regulation of KCNQ channels: biophysical and molecular mechanisms for lipid modulation of voltage-dependent gating. *Front. Physiol.* 5:195. https://doi.org/10.3389/fphys.2014.00195

Zolles, G., N. Klöcker, D. Wenzel, J. Weisser-Thomas, B.K. Fleischmann, J. Roeper, and B. Fakler. 2006. Pacemaking by HCN channels requires interaction with phosphoinositides. *Neuron.* 52:1027–1036. https://doi.org/10.1016/j.neuron.2006.12.005

Supplemental material

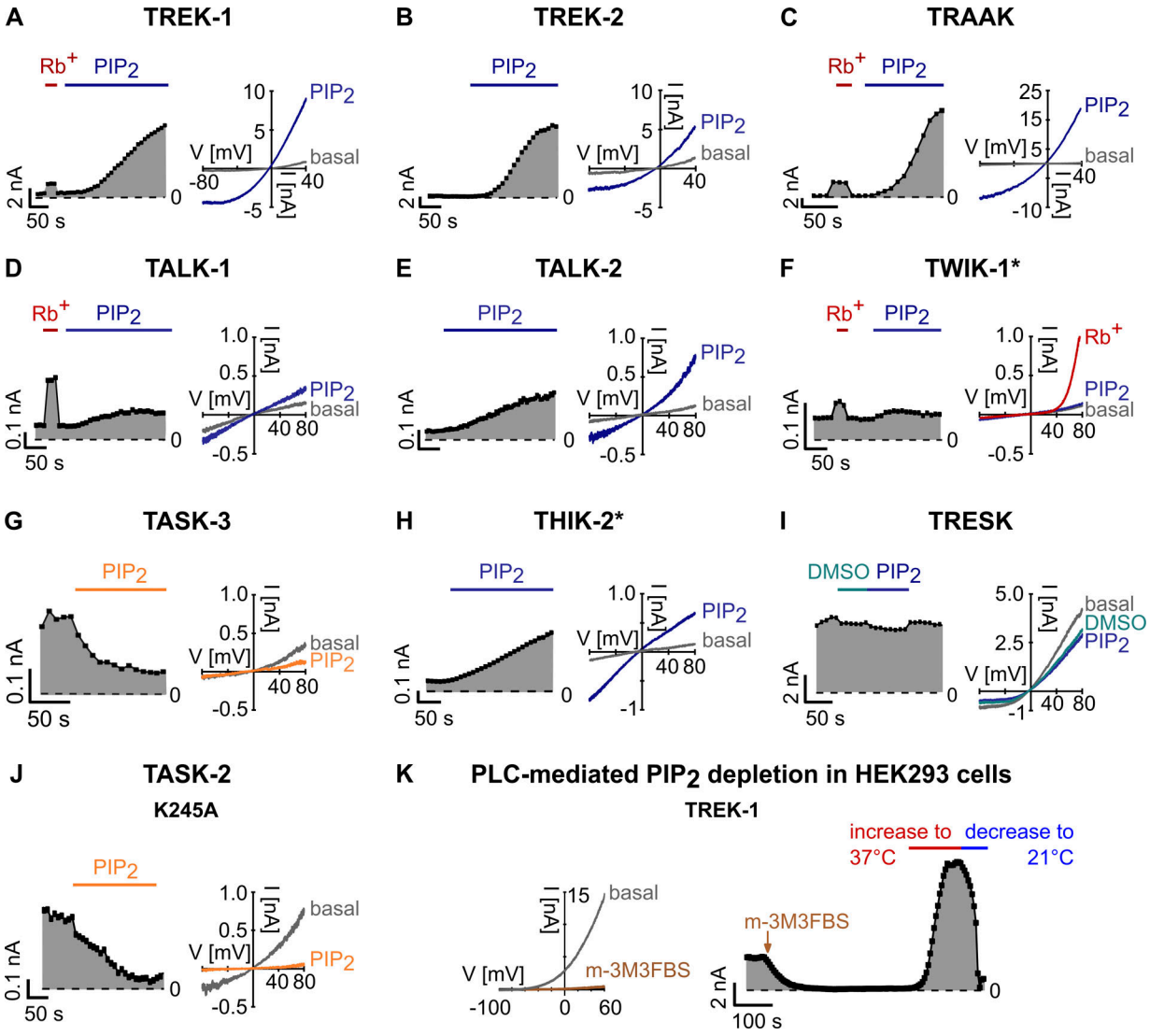

Figure S1. **Representative traces of the PIP_2 regulation of K_{2P} channels and PLC-mediated inhibition of TREK-1 channels. (A–J)** Representative current traces (right) and analyzed currents at +40 mV plotted over time (left) of PIP_2-activated (blue) TREK-1 (A), TREK-2 (B), TRAAK (C), TALK-1 (D), TALK-2 (E), THIK-2*- and PIP_2-inhibited (orange) TASK-3 (G), and TASK-2 K245A (J) K_{2P} channels. TWIK-1* (F) and TRESK (I) are not affected by PIP_2. Currents were measured in voltage ramps between −80 and +80 mV in excised inside-out patches of *Xenopus* oocytes using K^+ or Rb^+ (red) bath solutions and in the presence of 10 µM PIP_2 or DMSO (1%) added to the standard K^+ solution. **(K)** Representative traces of TREK-1 currents in whole-cell experiments using HEK293 cells measured in voltage ramps between −100 and +60 mV and analyzed at 0 mV. Measurements were performed in control solution and in the presence of 20 µM of the PLC activator m-3M3FBS. Additionally, the temperature was increased to 37°C (red) and subsequently decreased (blue) to room temperature of 21°C (blue).

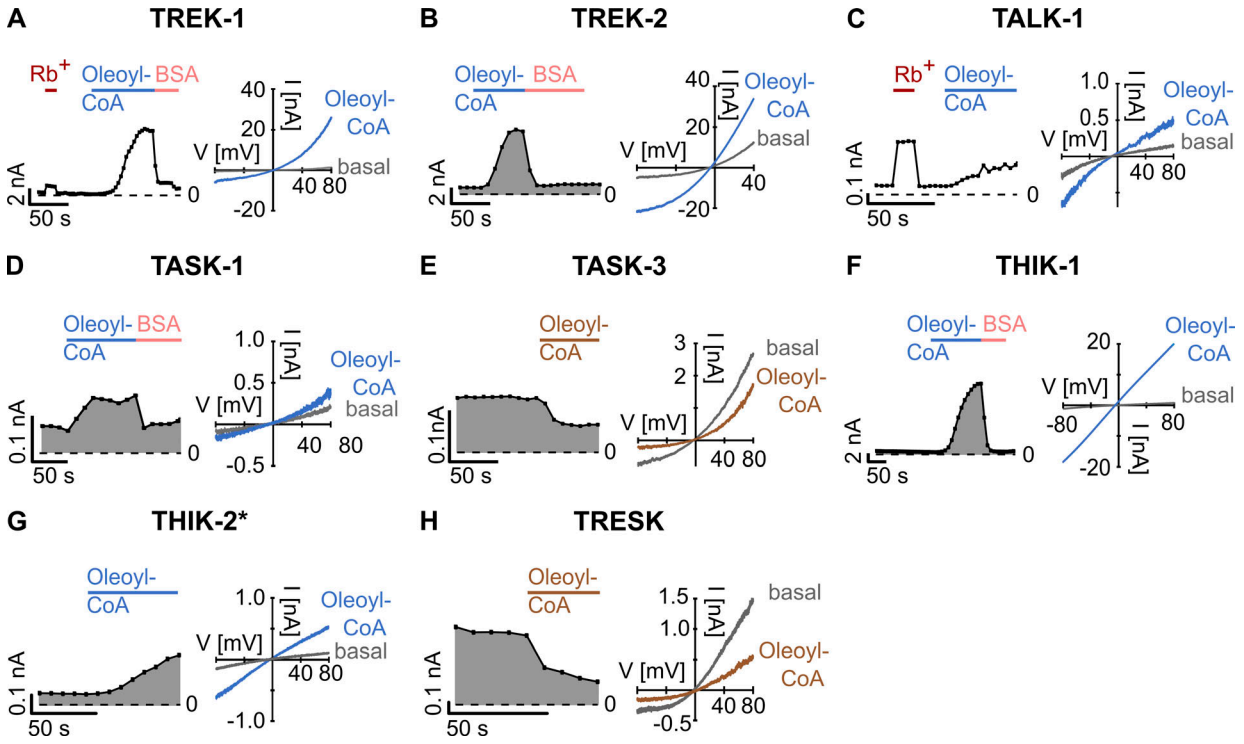

Figure S2. **Oleoyl-CoA regulation of K_{2P} channels. (A–H)** Representative current traces (right) and analyzed currents at +40 mV plotted over time (left) of oleoyl-CoA–activated (light blue) TREK-1 (A), TREK-2 (B), TALK-1 (C), TASK-1 (D), THIK-1 (F), and THIK-2* (G) and oleoyl-CoA–inhibited (brown) TASK-3 (E) and TRESK (H) K_{2P} channels. Currents were measured in voltage ramps between −80 and +80 mV in excised inside-out patches of *Xenopus* oocytes using K^+ or Rb^+ (red) bath solutions and in the presence of 10 µM PIP_2 or 5 mg ml^{-1} BSA (pink) added to the standard K^+ solution.

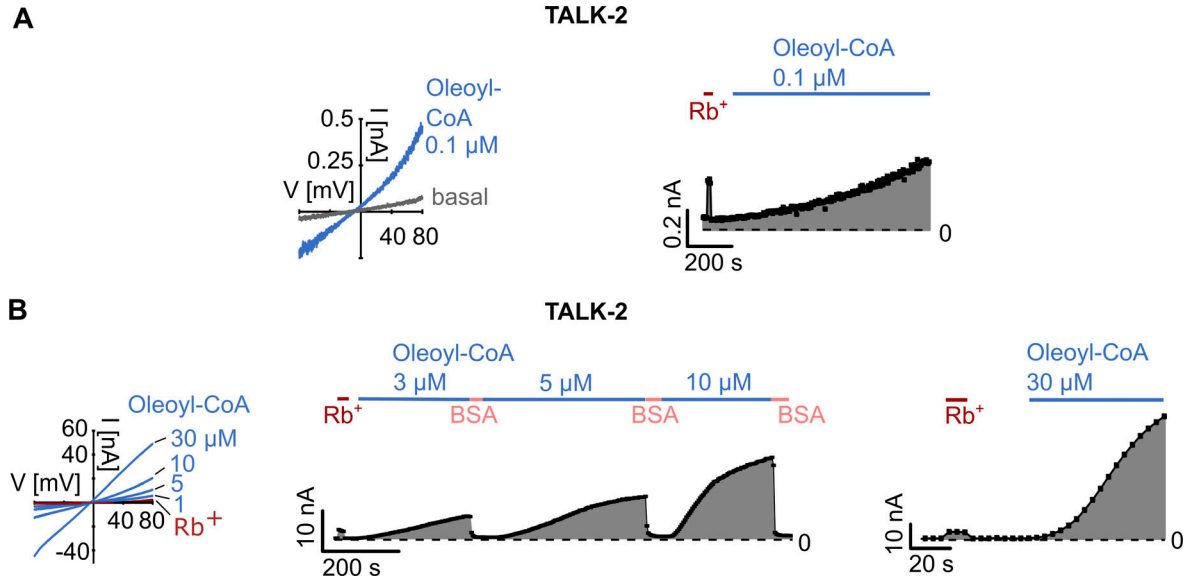

Figure S3. **Oleoyl-CoA activation of TALK-2 K_{2P} channels. (A and B)** Representative current traces (left) and analyzed currents at +80 mV plotted over time (right) of TALK-2 channels measured in voltage ramps between −80 and +80 mV in excised inside-out patches of *Xenopus* oocytes using K^+ or Rb^+ (red) bath solutions and in the presence of 0.1 µM (A), 1 µM, 3 µM, 5 µM, 10 µM, and 30 µM (B) oleoyl-CoA or 5 mg ml^{-1} BSA for washout.

Four tables are provided online. Table S1, Table S2, Table S3, and Table S4 contain the numerical data points depicted graphically in Fig. 1 A, Fig. 2 A, Fig. 3 D, and Fig. 4 C, respectively.